Available online at www.sciencedirect.com
SCIENCE DIRECT
Journal of Solid State Chemistry 179 (2006) 2047–2053
JOURNAL OF SOLID STATE CHEMISTRY
www.elsevier.com/locate/jssc

Structure and thermoelectric properties of the ordered skutterudite $CoGe_{1.5}Te_{1.5}$

Paz Vaqueiro[a,*], Gerard G. Sobany[a], A.V. Powell[a], Kevin S. Knight[b]

[a]*Department of Chemistry, Heriot-Watt University, Edinburgh EH14 4AS, UK*
[b]*ISIS Facility, Rutherford Appleton Laboratory, Didcot, Oxfordshire OX11 0QX, UK*

Received 27 February 2006; received in revised form 27 March 2006; accepted 2 April 2006
Available online 2 May 2006

Abstract

The skutterudite-related material $CoGe_{1.5}Te_{1.5}$ has been synthesised and structurally characterised by powder neutron diffraction. Analysis of the high-resolution powder neutron diffraction data indicates that the structure of $CoGe_{1.5}Te_{1.5}$ retains the $a^+a^+a^+$ tilt system of the ideal skutterudite structure, while the anions are ordered in layers perpendicular to the [111] direction of the skutterudite unit cell. This anion ordering results in a lowering of the symmetry from cubic to rhombohedral (space group $R\bar{3}$, $a = 12.3270(5)$ and $c = 15.102(1)$ Å at 293 K). The electrical transport properties have been investigated using four-probe resistivity and Seebeck coefficient measurements. The temperature dependence of the electrical resistivity and the magnitude of the Seebeck coefficient indicate that $CoGe_{1.5}Te_{1.5}$ is an n-type semiconductor.

Keywords: Skutterudite; Thermoelectric properties; Neutron diffraction

1. Introduction

Thermoelectric devices can be used for cooling applications or for power generation from a heat source. Although such devices offer considerable advantages over conventional systems, their use to date has been limited by their low efficiencies, which are determined by the performance of their constituent materials. The usefulness of a material for thermoelectric applications at a given temperature (T), is a function of its Seebeck coefficient (S), electrical resistivity (ρ), and thermal conductivity (κ), and can be evaluated using the figure of merit, $ZT = S^2T/\rho\kappa$ [1]. The difficulties in finding good thermoelectric materials arise from the fact that the materials are required to exhibit an unusual combination of low thermal conductivity, low electrical resistivity and high Seebeck coefficient. Recent experimental results on materials with the skutterudite structure demonstrate that these compounds possess attractive thermal and electrical transport properties for thermoelectric applications [2].

The ideal skutterudite structure (space group $Im\bar{3}$) can be described as a severe distortion of the ReO_3 structure by octahedron tilting (tilt system $a^+a^+a^+$) [3], in which the cations retain sixfold coordination while the anions form four-membered rings (Fig. 1). Binary skutterudites, which are compounds with composition MX_3 (M = Co, Rh or Ir and X = P, As or Sb) [4] have been widely investigated [2]. Our recent efforts have centred on the preparation and characterisation of ternary skutterudites, that are isoelectronic to the binary skutterudites. Ternary skutterudites can be obtained either by substitution at the anion site, X, by a pair of elements from groups 14 and 16 (e.g. $CoGe_{1.5}S_{1.5}$) [5], or by isoelectronic substitution at the cation site, M, by a pair of elements from groups 8 and 10 (e.g. $Fe_{0.5}Ni_{0.5}Sb_3$) [6]. Although a number of ternary skutterudites have been reported [5–10], there has been little work to date on the structural and physical properties of these materials. While ternary skutterudites formed by cation substitution appear to be isostructural to the binary skutterudites [6,9], structural studies carried out on two materials prepared by anion substitution, $CoGe_{1.5}S_{1.5}$ and $CoGe_{1.5}Se_{1.5}$ [5,11], suggest that these compounds crystallise in a modification of the skutterudite structure.

*Corresponding author. Fax: +44 131 451 3180.
E-mail address: chepv@hw.ac.uk (P. Vaqueiro).

0022-4596/$ - see front matter © 2006 Elsevier Inc. All rights reserved.
doi:10.1016/j.jssc.2006.04.004

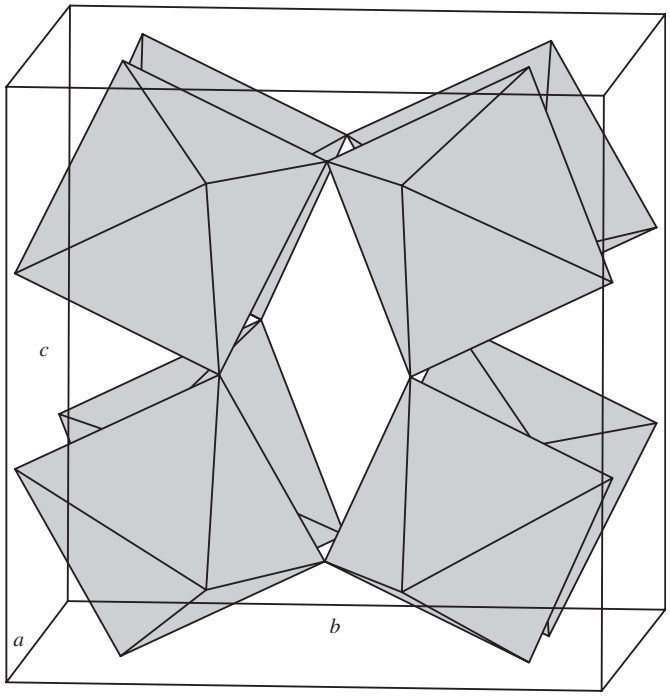

(a)

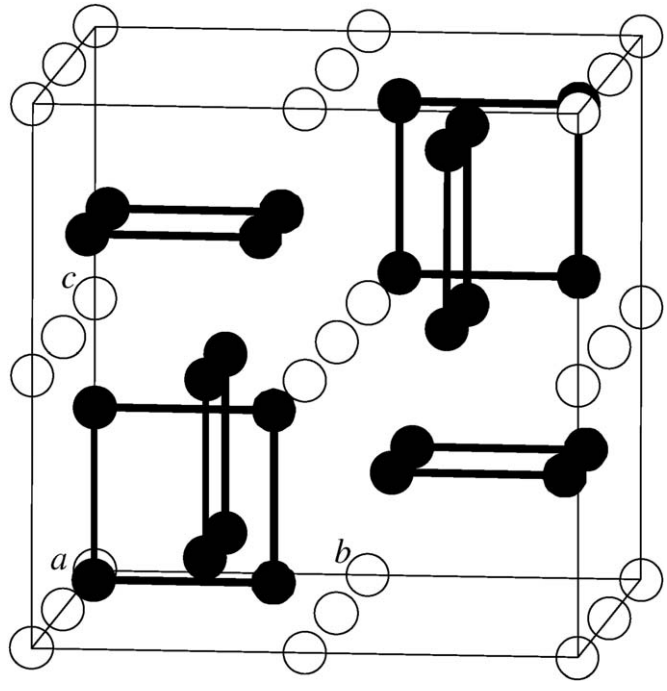

(b)

Fig. 1. Two representations of the skutterudite structure of MX_3: (a) polyhedral representation, showing the corner sharing MX_6 octahedra. (b) Ball and stick representation, showing the planar rectangular four-membered X_4 rings. Key: M, open circles; X, black circles.

Korestein et al. [5] reported that the structure of $CoGe_{1.5}S_{1.5}$ could be described by taking into account short-range ordering of the anions, whilst Partik et al. [11] carried out a single crystal study on twinned crystals of $CoGe_{1.5}Q_{1.5}$ (Q = S, Se) and reported that the Ge and Q atoms exhibit long-range ordering, which results in a lowering of the symmetry from cubic to rhombohedral. This conclusion is supported by infra-red spectra of the ternary skutterudites $MGe_{1.5}Q_{1.5}$ (M = Co, Ir, Q = S, Se), which exhibit a large number of lattice vibration modes when compared with binary skutterudites, consistent with a lowering of the cubic symmetry [8]. Table 1 summarises the known ternary skutterudites obtained by isoelectronic substitution at the anion site. To our knowledge, the only available structural studies on ternary skutterudites are those described above [5,11], and the structure of the remaining materials has not been investigated.

Table 1
Known ternary skutterudites obtained by substitution at the anion site, and their lattice parameters calculated on the basis of a primitive cubic unit cell

Material	Lattice parameter (Å)	Literature ref.
$CoGe_{1.5}S_{1.5}$	8.017	[5]
$CoGe_{1.5}Se_{1.5}$	8.299	[5]
$CoGe_{1.5}Te_{1.5}$	8.7270	[10]
$CoSn_{1.5}Se_{1.5}$	8.7959	[10]
$CoSn_{1.5}Te_{1.5}$	9.1284	[10]
$RhGe_{1.5}S_{1.5}$	8.2746	[7]
$RhGe_{1.5}Se_{1.5}$	8.546	[8]
$IrGe_{1.5}S_{1.5}$	8.2970	[7]
$IrGe_{1.5}Se_{1.5}$	8.5591	[7]
$IrSn_{1.5}S_{1.5}$[a]	8.7059	[7]
$IrSn_{1.5}Se_{1.5}$	8.9674	[10]
$IrSn_{1.5}Te_{1.5}$	9.3320	[10]

[a]Material prepared at high pressures (40 kbar).

In this work, we present a detailed structural study on the ternary skutterudite $CoGe_{1.5}Te_{1.5}$ using high-resolution powder neutron diffraction, together with measurements of the transport properties over the temperature range $77 \leqslant T(K) \leqslant 300$.

2. Experimental

A mixture of cobalt (Aldrich, 99.9%), germanium (Aldrich, 99.99%) and tellurium (Aldrich, 99.997%) powders corresponding to the stoichiometry $CoGe_{1.5}Te_{1.5}$ was ground in an agate mortar prior to sealing into an evacuated ($<10^{-4}$ Torr) silica tube. The mixture was heated at 1 °C min^{-1} to 500 °C for 24 h, 600 °C for 4 days and then cooled to room temperature at 0.5 °C min^{-1} prior to removal from the furnace. Following re-grinding, the material was sealed into a second silica tube and refired at 600 °C for 3 days, and cooled to room temperature at 0.1 °C min^{-1}. The sample was initially characterised using powder X-ray diffraction, collected on a Philips PA2000 diffractometer with nickel-filtered Cu$K\alpha$ radiation ($\lambda = 1.5418$ Å). For transport property measurements, pellets of $CoGe_{1.5}Te_{1.5}$ were cold pressed, sealed into an evacuated silica tube, heated at 600 °C for 1 day and then cooled to room temperature at 0.1 °C min^{-1}. Analytical

electron microscopy on the powdered sample was performed using a Philips XL30CP scanning microscope, equipped with an EDAX PGT Spirit detection system. The experimentally determined Co:Ge and Te:Ge ratios are 0.67(4) and 1.39(7), which result in a composition $Co_{1.00}Ge_{1.48}Te_{2.07}$. While there is a very good agreement in the Co:Ge ratio, there are significant deviations in the Te:Ge ratio, arising as a consequence of small grain sizes ($<5\,\mu m$), which can introduce large deviations in the relative intensities measured by EDAX when analysing elements with significantly different atomic numbers [12].

Time-of-flight powder neutron diffraction data were collected on the HRPD diffractometer at ISIS, Rutherford Appleton Laboratory. The sample was contained in a vanadium can, and data were collected at 4.2 and 293 K. Initial data manipulation and reduction was carried out using Genie [13] spectrum manipulation software. Neutron diffraction data from the backscattering and 90° detector banks were summed, normalised and used simultaneously in Rietveld refinements, which were performed using the GSAS package [14].

The electrical resistance of the sample as a function of temperature was measured using the four-probe DC technique. An ingot ($\sim 6\times3\times1$ mm) was cut from a sintered pellet, four 50 μm silver wires were attached using colloidal silver paint and connexions were made to a HP34401A multimeter. The sample was mounted in an Oxford Instruments CF1200 cryostat connected to an ITC502 temperature controller. Measurements were carried out over the temperature range $77\leqslant T(K)\leqslant300$. For Seebeck measurements, an ingot ($\sim10\times4\times1$ mm) was cut from a sintered pellet. This was then mounted on a sample stick designed and built *in-house*, which includes a small heater located close to one end of the sample, thus allowing a temperature gradient to be applied to the sample. Two 50 μm copper wires were attached to the ends of the sample, and connexions made to a Keithley 2182 nanovoltmeter. Two Au:0.07%Fe vs. chromel thermocouples were placed in contact with the sample at the hot and cold ends, and connected to an ITC503 temperature controller (Oxford Instruments). The sample stick was placed in an Oxford Instruments CF1200 cryostat connected to an ITC502 temperature controller. The Seebeck coefficient, at a given temperature, was determined by sweeping a temperature gradient, ΔT, and measuring the corresponding thermal voltage, ΔV [15]. In this manner, the slope of the line, $\Delta V/\Delta T$, can be used to determine the Seebeck coefficient, rendering offset voltages due to instrumentation inconsequential. Measurements were carried out over the temperature range $77\leqslant T(K)\leqslant300$, in 5 K steps.

3. Results and discussion

3.1. Structure of $CoGe_{1.5}Te_{1.5}$

With the exception of a small number of weak features attributable to $CoTe_2$ (ca. 4%) and GeO_2 (ca. 1%) impurity phases, the powder neutron diffraction patterns of $CoGe_{1.5}Te_{1.5}$ can be indexed on the basis of a primitive cubic unit cell, with the intense reflections corresponding to the skutterudite body-centred condition $h+k+l=2n$. There are a number of weaker reflections present in the patterns, which violate the body-centred reflection condition of the skutterudite (space group $Im\bar{3}$), while the absence of peak splittings suggests that a cubic unit cell is retained. However structural models for the skutterudite phase based on cubic subgroups of $Im\bar{3}$ (such as $Pm\bar{3}$ or $P23$) failed to reproduce adequately the observed intensities. While the structure of $CoGe_{1.5}Te_{1.5}$ is metrically cubic, like the analogous $CoGe_{1.5}Q_{1.5}$ ($Q=$ S, Se) [5,11], the lattice parameters of ternary skutterudites containing heavier transition metals, such as $RhGe_{1.5}Q_{1.5}$ ($Q=$ S, Se) [8], have been reported to exhibit small deviations from the pseudo-cubic unit cell. Since metric symmetry in perovskite-related structures is sometimes higher than that of the space group, Rietveld refinements using the model of anion ordering proposed by Partik et al. [11] for $CoGe_{1.5}Se_{1.5}$ (space group $R3$), were carried out. Although these refinements resulted in a good agreement between observed and calculated intensities, they failed to reach convergence. Use of Platon/Addsym to identify missing symmetry elements [16,17], both in the reported structure of $CoGe_{1.5}Se_{1.5}$ [11] and in our refined model for $CoGe_{1.5}Te_{1.5}$ (space group $R3$), indicated clearly that there was a centre of inversion missing, and that therefore the structure of these materials should be better described in the centrosymmetric space group $R\bar{3}$. The relationship between the parent space group ($Im\bar{3}$) and $R3$ and $R\bar{3}$ was explored by means of a group-theoretical analysis, performed using isotropy [18]. This resulted in the identification of the isotropy subgroups of $Im\bar{3}$, each of which consists of all space-group elements of the parent group which leave the order parameter invariant for a given distortion. This analysis indicated that, for units cells of the same size than the original cell, $R3$ is not an isotropy subgroup of $Im\bar{3}$, while $R\bar{3}$ is one of the isotropy subgroups for the irreducible representation H_4^+ ($\mathbf{k}=(1,1,1)$) which can be associated with anion ordering along the [111] direction of the original unit cell. Furthermore, $R\bar{3}$ is the only one of the isotropy subgroups which shows the full symmetry (*a, a, a*) of the anion ordering. This analysis confirms our findings using Platon and let us to conclude that the structure of $CoGe_{1.5}Te_{1.5}$ is correctly described in the space group $R\bar{3}$. The refined parameters for the structure of $CoGe_{1.5}Te_{1.5}$ in the space group $R\bar{3}$ are presented in Table 2 and final observed, calculated and difference profiles for the neutron data at 4.2 K are shown in Fig. 2. Selected distances and angles are given in Table 3. Refinements were carried out using an overall thermal parameter. Refinement of all the atom coordinates using the data collected at 4.2 K indicated that while the anion sublattice is distorted when compared with the skutterudite structure, the cation coordinates do not deviate significantly from their ideal positions. Therefore, in the refinement using the 293 K data, for which a shorter

Table 2
Refined parameters for $CoGe_{1.5}Te_{1.5}$ determined from data collected at 4.2 and 293 K on HRPD (space group $R\bar{3}$)

		Temperature (K)	
		4.2	293
a (Å)		12.3009(3)	12.3270(5)
c (Å)		15.0678(8)	15.102(1)
B (Å^2)		0.099(2)[a]	0.186(5)[a]
Co(1)	x	0	0
	y	0	0
	z	0.247(6)	1/4(—)[b]
Co(2)	x	0.668(6)	2/3(—)[b]
	y	0.832(4)	5/6(—)[b]
	z	0.581(2)	7/12(—)[b]
Ge(1)	x	0.835(1)	0.835(2)
	y	0.9935(8)	0.993(1)
	z	0.1599(8)	0.161(1)
Ge(2)	x	0.946(1)	0.946(2)
	y	0.217(2)	0.217(2)
	z	0.5550(5)	0.5557(8)
Te(1)	x	0.934(1)	0.935(2)
	y	0.213(2)	0.212(3)
	z	0.0668(8)	0.065(1)
Te(2)	x	0.836(2)	0.837(3)
	y	0.013(1)	0.014(2)
	z	0.665(1)	0.667(2)
R_{wp} (backscattering bank) (%)		2.4	6.9
R_{wp} (90° bank) (%)		1.9	6.1
χ^2		4.7	2.1

All atoms on 18(*f*): (*x,y,z*), except for Co(1) on 6(*c*): (*0,0,z*).
[a]Thermal parameters were constrained to be equal for all the atoms.
[b]Non-refined variables (see text).

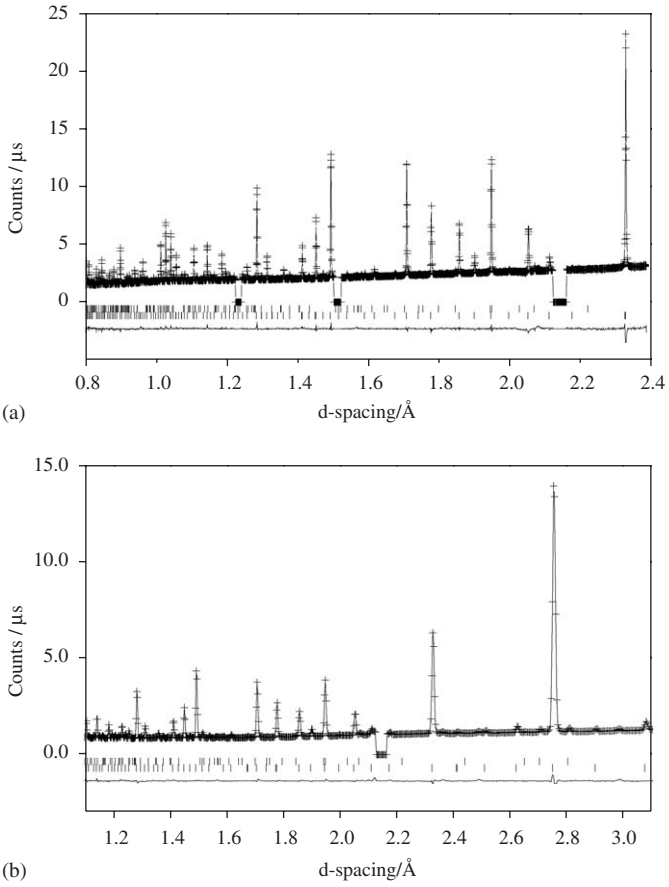

Fig. 2. Final observed (crosses), calculated (full line) and difference (lower full line) neutron profiles for $CoGe_{1.5}Te_{1.5}$ collected on the HRPD diffractometer at 4.2 K. Reflection positions are marked: the lower markers refer to $CoGe_{1.5}Te_{1.5}$ and the upper markers to $CoTe_2$.

collection time was employed, the cation coordinates were fixed at their ideal positions.

The structure of $CoGe_{1.5}Te_{1.5}$ can be described as an infinite array of distorted and tilted octahedra, with each octahedron sharing corners with six neighbouring octahedra. This structure retains the $a^+a^+a^+$ tilt system of the parent skutterudite structure, while the anions are ordered in layers perpendicular to the [111] direction of the skutterudite unit cell. This corresponds to the *c*-axis of the $R\bar{3}$ cell in the hexagonal setting. Each cobalt cation is octahedrally coordinated by three germanium and three tellurium anions, with average Co–Ge and Co–Te distances of 2.39 and 2.48 Å (at 293 K), respectively, comparable to those observed in binary cobalt germanides [19] and tellurides [20]. *X–M–X* angles in $CoGe_{1.5}Te_{1.5}$, which lie in the range 82.4(6)–97.1(8), show significant deviations from ideal octahedral geometry. When compared with binary skutterudites such as $CoSb_3$ [21], in which all the *M–X* distances are identical (but *X–M–X* angles deviate from 90°), the octahedra in the $CoGe_{1.5}Te_{1.5}$ structure are more distorted. Owing to the tilting of the octahedra, the anions form two-crystallographically distinct four-membered rings, with stoichiometry $[Ge_2Te_2]^{4-}$, in which the germanium and tellurium atoms are *trans* to each other (Fig. 3). In binary skutterudites such as $CoSb_3$, there is only one crystallographically distinct Sb_4^{4-} ring, of rectangular shape, in which short and long Sb–Sb distances alternate (Fig. 4(a)). This contrasts with the $[Ge_2Te_2]^{4-}$ rings in $CoGe_{1.5}Te_{1.5}$, in which short and long Ge–Te distances alternate but the angles deviate from 90° (Fig. 4(b)). In addition to the short intraring Ge–Te distances (< 3 Å), each atom of a $[Ge_2Te_2]^{4-}$ ring has two contacts (ca. 3.3 Å) with every adjacent ring, at distances substantially shorter than the sum of the van der Waals' radii [22]. Band structure calculations on binary skutterudites indicate that the contribution of these interring contacts to the density of states is significant [23].

Other ternary skutterudites prepared by anion substitution might also exhibit an ordered skutterudite structure, involving anion ordering and distortion of the square planar rings, and this might account for their typically low thermal conductivities when compared with binary skutterudites.

3.2. Transport properties of $CoGe_{1.5}Te_{1.5}$

The electrical resistivity of $CoGe_{1.5}Te_{1.5}$ increases with decreasing temperature, indicating that this material is a

Table 3
Selected bond distances (Å) and angles (°) for $CoGe_{1.5}Te_{1.5}$

	Temperature (K)	
	4.2	293
Bond		
Co(1)–Ge(1)	3 × 2.39(5)	3 × 2.40(2)
Co(1)–Te(2)	3 × 2.48(5)	3 × 2.45(3)
Co(2)–Ge(1)	2.31(5)	2.35(1)
Co(2)–Ge(2)	2.36(4)	2.39(2)
Co(2)–Ge(2)	2.39(4)	2.42(1)
Mean Co(2)–Ge	2.35(4)	2.39(1)
Co(2)–Te(1)	2.52(4)	2.50(2)
Co(2)–Te(1)	2.53(4)	2.49(3)
Co(2)–Te(2)	2.49(4)	2.51(3)
Mean Co(2)–Te	2.51(4)	2.50(2)
Angle		
Ge(1)–Co(1)–Ge(1)	3 × 92.5(3)	3 × 91.8(7)
Te(2)–Co(1)–Te(2)	3 × 94.2(3)	3 × 96.0(8)
Ge(1)–Co(1)–Te(2)	3 × 90.3(6)	3 × 89.9(7)
Ge(1)–Co(1)–Te(2)	3 × 83.2(4)	3 × 82.4(6)
Ge(1)–Co(2)–Ge(2)	89.5(6)	88.9(5)
Ge(1)–Co(2)–Ge(2)	87.9(9)	86.7(4)
Ge(2)–Co(2)–Ge(2)	94.3(2)	92.9(8)
Te(1)–Co(2)–Te(1)	94.4(2)	94.9(1)
Te(1)–Co(2)–Te(2)	82.8(8)	83.8(8)
Te(1)–Co(2)–Te(2)	84.6(6)	85.6(6)
Ge(1)–Co(2)–Te(1)	97.1(2)	97.1(8)
Ge(1)–Co(2)–Te(1)	89.5(2)	89.5(6)
Te(1)–Co(2)–Ge(2)	89.0(8)	88.8(7)
Te(2)–Co(2)–Ge(2)	96.4(2)	83.5(7)
Te(2)–Co(2)–Ge(2)	94.3(2)	95.8(8)
Te(2)–Co(2)–Ge(2)	91.8(2)	92.3(7)

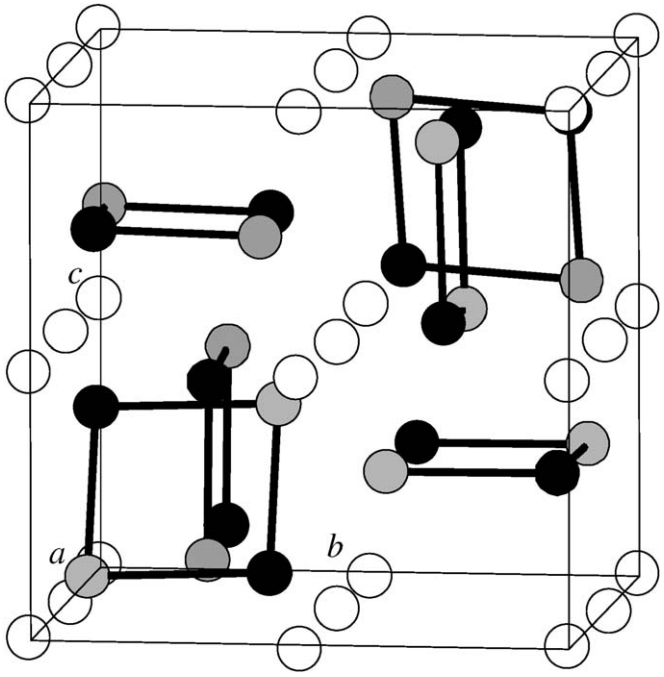

Fig. 3. Representation of the structure of the skutterudite-related $CoGe_{1.5}Te_{1.5}$ showing the anion ordering. For comparison purposes with Fig. 1, the rhombohedral setting of $CoGe_{1.5}Te_{1.5}$ has been used. Key: cobalt, open circles; tellurium, black circles and germanium, grey circles.

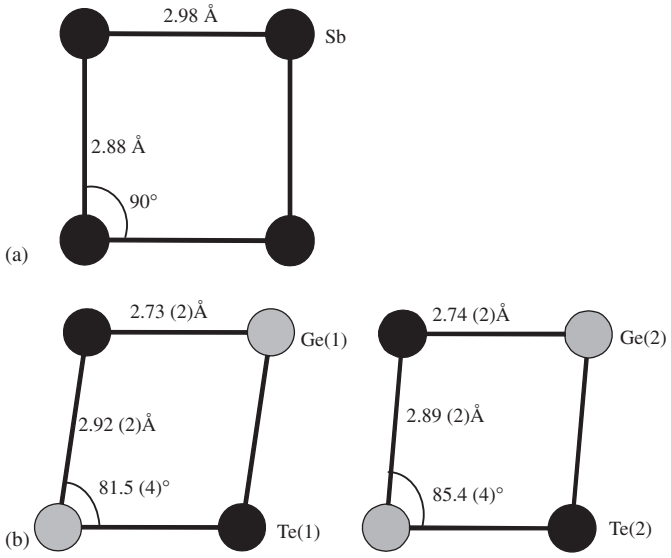

Fig. 4. The four-membered rings in: (a) $CoSb_3$ [21] and (b) $CoGe_{1.5}Te_{1.5}$.

semiconductor (Fig. 5(a)). The activation energy over the temperature range $140 \leqslant T(K) \leqslant 300$, determined using an Arrhenius law, is 0.16(1) eV, comparable to that reported by Navratil et al. [24]. This value is similar to the activation energies determined for the ternary skutterudites $IrGe_{1.5}S_{1.5}$ (0.11 eV) [7], $IrGe_{1.5}Se_{1.5}$ (0.076 eV) [7] and $CoGe_{1.5}Se_{1.5}$ (0.17 eV) [25] over comparable temperature ranges. It has been suggested that this energy represents the activation energy of the extrinsic charge carriers, and therefore measurements at elevated temperatures may be required to determine the intrinsic band gap. Over the entire temperature range, $CoGe_{1.5}Te_{1.5}$ has a markedly higher electrical resistivity ($\rho = 5.1\,\Omega\,cm$ at room temperature) than binary skutterudites such as $CoSb_3$ ($\rho = 1.9 \times 10^{-3}\,\Omega\,cm$) [26]. This is consistent with the higher electrical resistivities observed for other ternary skutterudites, such as $CoGe_{1.5}Se_{1.5}$ [25] or $CoSn_{1.5}Te_{1.5}$ [27]. Although the higher resistivity has been attributed to lower charge-carrier mobilities, the charge-carrier density will also play a key rôle in determining the magnitude of the resistivity: further studies are required to establish the optimum doping level. The lower charge-carrier mobility might be related to the larger electronegativity differences between the constituent elements in ternary skutterudites, when compared with binary skutterudite antimonides. It has been argued that while in purely covalent lattices carrier mobility is high, in materials containing elements with different electronegativities, charge fluctuations from atom to atom increase the charge-carrier scattering and therefore decrease the mobility [28].

The magnitude of the Seebeck coefficient of $CoGe_{1.5}Te_{1.5}$ is consistent with semiconducting behaviour ($S = -697\,\mu V\,K^{-1}$ at 273 K), and its negative values indicate that the majority of the charge carriers are electrons (Fig. 5(b)). The temperature dependence of the

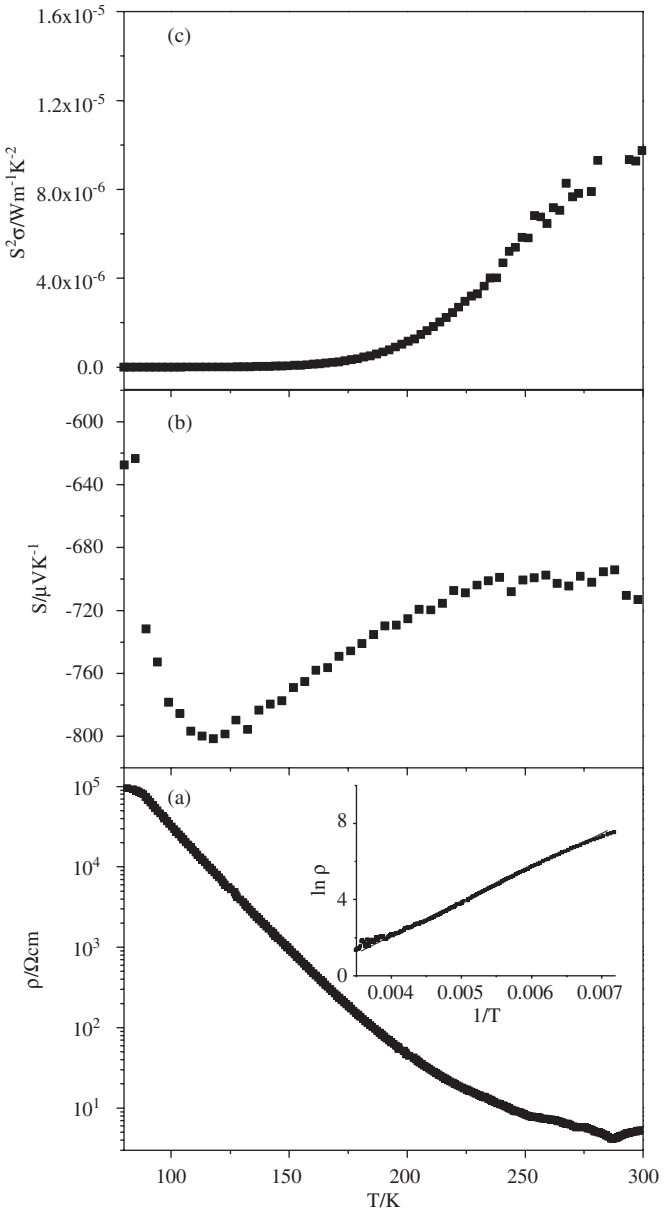

Fig. 5. Temperature dependence of: (a) the electrical resistivity; (b) the Seebeck coefficient and (c) the power factor of $CoGe_{1.5}Te_{1.5}$. The inset shows $\ln\rho$ vs. the inverse of temperature over the temperature range $140 \leqslant T(K) \leqslant 300$.

Seebeck coefficient is similar to that observed for n-type $CoGe_{1.5}Se_{1.5}$, except that the temperature at which the Seebeck coefficient reaches a minimum value is 115 K for $CoGe_{1.5}Te_{1.5}$ and ca. 150 K for $CoGe_{1.5}Se_{1.5}$ [25]. It has been suggested that at low carrier concentration levels, impurity band conduction may play an important role in the electrical transport at low temperatures, and in lightly doped $CoSb_3$ samples, the temperature dependence of the Seebeck coefficient has been accounted for using a two-band model consisting of the conduction band and an impurity band [29].

The power factor of $CoGe_{1.5}Te_{1.5}$ as a function of temperature is shown in Fig. 5(c). In the studied temperature range, the power factor increases with increasing temperature, reaching a value of ca. $1 \times 10^{-5}\,W\,m^{-1}\,K^{-2}$ at 300 K. This value is comparable to that reported for other ternary skutterudites [25,27], but significantly lower than the power factors found in state-of-the-art thermoelectric materials. However, the large Seebeck coefficient of $CoGe_{1.5}Te_{1.5}$ makes it interesting for further investigation, which will include doping to optimise the number of charge carriers and void filling to decrease the thermal conductivity. This might result in improved thermoelectric properties.

Acknowledgments

We acknowledge financial support for this work from the UK EPSRC. PV thanks the UK EPSRC for an Advanced Research Fellowship.

References

[1] F.J. DiSalvo, Science 285 (1999) 703.
[2] C. Uher, in: M.G. Kanatzidis, S.D. Mahanti, T.P. Hogan (Eds.), Chemistry, Physics and Materials Science of Thermoelectric Materials: Beyond Bismuth Telluride, Kluwer Academics/Plenum Publishers, New York, 2003, p. 121.
[3] R.H. Mitchell, Perovskites: Modern and Ancient, Almaz Press, Ontario, Canada, 2002.
[4] A. Kjeksus, D.G. Nicholson, T. Rakke, Acta Chem. Scand. 27 (1973) 1307.
[5] R. Korestein, S. Soled, A. Wold, G. Collin, Inorg. Chem. 16 (1977) 2344.
[6] A. Kjeshus, D.G. Nicholson, T. Rakke, Acta Chem. Scand. 27 (1973) 1315.
[7] A. Lyons, R.P. Gurska, C. Case, S.N. Subbarao, A. Wold, Mater. Res. Bull. 13 (1978) 125.
[8] H.D. Lutz, G. Kliche, J. Solid State Chem. 40 (1981) 64.
[9] T. Caillat, J. Kullet, A. Borshchevsky, J.-P. Fleurial, J. Appl. Phys. 79 (1996) 8419.
[10] J.-P. Fleurial, T. Caillat, A. Borshchevsky, Proceedings of the 16th International Conference on Thermoelectrics, Dresden, Germany, 1997, p. 1.
[11] M. Partik, C. Kringe, H.D. Lutz, Z. Kristallogr. 211 (1996) 304.
[12] J.I. Goldstein, D.E. Newbury, P. Echlin, D.C. Coy, C. Fiori, E. Lifshin, Scanning Electron Microscopy and X-Ray Microanalysis, Plenum Press, New York, 1981.
[13] W.I.F. David, M.W. Johnson, K.J. Knowles, C.M. Moreton-Smith, G.D. Crisbie, E.P. Campbell, S.P. Graham, J.S. Lyall, Rutherford Appleton Laboratory Report, RAL-86-102, 1986.
[14] A.C. Larson, R.B. von Dreele, General Structure Analysis System, Report LAUR 85-748, Los Alamos Laboratory, 1994.
[15] G.R. Caskey, D.J. Sellmyer, L.G. Rubin, Rev. Sci. Instr. 40 (1969) 1280.
[16] A.L. Spek, J. Appl. Crystallogr. 36 (2003) 7.
[17] A.L. Spek, J. Appl. Crystallogr. 21 (1988) 578.
[18] C.J. Howard, H.T. Stokes, Acta Crystallogr. A 61 (2005) 93.
[19] M. Ellner, J. Less-Common Met. 48 (1976) 21.
[20] M. Muhler, W. Bensch, M. Schur, J. Phys.: Condens. Matter 10 (1998) 2947.
[21] Th. Schmidt, G. Kliche, H.D. Lutz, Acta Crystallogr. C 43 (1987) 1678.
[22] A. Bondi, J. Phys. Chem. 68 (1964) 441.

[23] D. Jung, M.-H. Whangbo, S. Alvarez, Inorg. Chem. 29 (1990) 2252.
[24] J. Navrátil, T. Plecháček, L. Beneš, M. Vlček, J. Optoelectron. Adv. Mater. 6 (2004) 787.
[25] G.S. Nolas, J. Yang, R.W. Ertenberg, Phys. Rev. B 68 (2003) 193206.
[26] T. Caillat, A. Borshchevsky, J.-P. Fleurial, J. Appl. Phys. 80 (1996) 4442.
[27] Y. Nagamoto, K. Tanaka, T. Koyanagi, Proceedings of the 16th International Conference on Thermoelectrics, 1997, Dresden, Germany, p. 330.
[28] G.A. Slack, in: D.M. Rowe (Ed.), CRC Handbook of Thermoelectrics, Chemical Rubber, Boca Raton, FL, 1995 (Chapter 34).
[29] J.S. Dyck, W. Chen, J. Yang, G. P Meisner, C. Uher, Phys. Rev. B 65 (2002) 115204.